Scapular kinematics during manual wheelchair propulsion in able-bodied participants

Bekker, Michel J.; Vegter, Riemer J.K.; van der Scheer, Jan W.; Hartog, Johanneke; de Groot, Sonja; de Vries, Wiebe; Arnet, Ursina; van der Woude, Lucas H.V.; Veeger, Dirkjan (.H.E.J)

published in
Clinical Biomechanics
2018

DOI (link to publisher)
10.1016/j.clinbiomech.2018.03.008

document version
Publisher's PDF, also known as Version of record

document license
Article 25fa Dutch Copyright Act

Clinical Biomechanics 54 (2018) 54–61

Contents lists available at ScienceDirect

Clinical Biomechanics

journal homepage: www.elsevier.com/locate/clinbiomech

Lecture

Scapular kinematics during manual wheelchair propulsion in able-bodied participants

Michel J. Bekker[a,b,c,*], Riemer J.K. Vegter[c], Jan W. van der Scheer[c], Johanneke Hartog[c,d], Sonja de Groot[c,e], Wiebe de Vries[a], Ursina Arnet[a,f], Lucas H.V. van der Woude[c,g], Dirkjan (.H.E.J). Veeger[b,h]

[a] Swiss Paraplegic Research, Guido A. Zächstrasse 4, CH, 6207 Nottwil, Switzerland
[b] Research Institute MOVE, Department of Human Movement Sciences, Free University Amsterdam, Van der Boechorststraat 7, NL, 1081BT Amsterdam, The Netherlands
[c] Center for Human Movement Sciences, University Medical Center Groningen, University of Groningen, Antonius Deusinglaan 1, NL-9713AV Groningen, The Netherlands
[d] Department of Cardiology and Thoracic Surgery, University Medical Center Groningen, University of Groningen, Hanzeplein 1, NL-9713GZ Groningen, The Netherlands
[e] Amsterdam Rehabilitation Research Center Reade, Dr. Jan van Breemenstraat 2, NL, 1056AB Amsterdam, The Netherlands
[f] University of Lucerne, Department of Health Sciences, Frohburgstrasse 3, CH, 6002 Lucerne, Switzerland
[g] Center for Rehabilitation, University Medical Center Groningen, University of Groningen, Antonius Deusinglaan 1, NL-9713AV Groningen, The Netherlands
[h] Department of Biomechanical Engineering, Delft University of Technology, Mekelweg 2, NL, 2628CD Delft, The Netherlands

ARTICLE INFO

Keywords:
Scapular kinematics
Biomechanics
Manual wheelchair propulsion

ABSTRACT

Background: Altered scapular kinematics have been associated with shoulder pain and functional limitations. To understand kinematics in persons with spinal cord injury during manual handrim wheelchair propulsion, a description of normal scapular behaviour in able-bodied persons during this specific task is a prerequisite for accurate interpretation. The primary aim of this study is to describe scapular kinematics in able-bodied persons during manual wheelchair propulsion.

Methods: Sixteen able-bodied, novice wheelchair users without shoulder complaints participated in the study. Kinematic and kinetic data were collected during a standardized pose in the anatomic posture, frontal-plane arm elevation and low-intensity steady-state handrim wheelchair propulsion and upper-body Euler angles were calculated.

Findings: Scapulothoracic joint orientations in a static position were 36.7° (SD 5.4°), 6.4° (SD 9.1°) and 9.1° (SD 5.7°) for respectively protraction, lateral rotation and anterior tilt. At 80° of arm elevation in the frontal plane, the respective values of 33.4° (SD 8.0°), 23.9° (SD 5.4°) and 4.1° (SD 11.3°) were found. During the push phase of manual wheelchair propulsion, the mean scapular rotations were respectively 32.7° (SD 7.1°), 7.1° (SD 9.2°) and 9.8° (SD 8.3°).

Interpretation: The orientation of the scapula in a static pose, during arm elevation and in manual wheelchair propulsion in able-bodied participants showed similar patterns to a previous study in persons with para- and tetraplegia. These values provide a reference for the investigation of the scapular movement pattern in wheelchair-dependent persons and its relation to shoulder complex abnormalities.

1. Introduction

In comparison to the general population, the prevalence of shoulder pain in persons with an SCI is high: around 30–70% (Curtis et al., 1995; Gironda et al., 2004; Turner et al., 2001) whereas in the general population it is estimated to be 7–27% (Luime et al., 2004).

Shoulder pain affects the quality of functioning and peak capacity of wheelchair-dependent persons with SCI during activities of daily life (Ballinger et al., 2000; Salisbury et al., 2003; Samuelsson et al., 2004). Considering that persons with SCI are highly dependent on their upper extremities for activities of daily life such as dressing, mobility and self-care (Eriks-Hoogland et al., 2011; van Drongelen et al., 2006), the impact of this pain can be substantial.

One of the possible factors contributing to musculoskeletal shoulder pain is subacromial impingement syndrome; a narrowing of the subacromial space leading to impingement and inflammation or even impairment of structures in the subacromial cavity, such as nerves, bursae and tendons (Finley et al., 2005). Subacromial impingement syndrome

* Corresponding author.
E-mail addresses: michel.bekker.work@gmail.com (M.J. Bekker), r.j.k.vegter@umcg.nl (R.J.K. Vegter), j.hartog@umcg.nl (J. Hartog), s.d.groot@reade.nl (S. de Groot), wiebe.devries@paraplegie.ch (W. de Vries), ursina.arnet@paraplegie.ch (U. Arnet), l.h.v.van.der.woude@umcg.nl (L.H.V. van der Woude), h.e.j.veeger@vu.nl (D. Veeger).

https://doi.org/10.1016/j.clinbiomech.2018.03.008
Received 20 October 2016; Accepted 13 March 2018

Glossary

AC	Acromioclavicular joint
ACD	Dorsal acromioclavicular joint
ACV	Ventral acromioclavicular joint
ACM	Acromion cluster marker
CV	Coefficient of variation
GH	Glenohumeral joint
ICC	Intraclass correlation
LCS	Local coordinate system
RMSE	Root mean square error
SC	Sternoclavicular joint
SCI	Spinal cord injury
ST	Scapulothoracic joint
TH	Thoracohumeral joint

has been closely related, either causative or compensational, to abnormal movement patterns of the scapula (increased medial rotation and anterior tilt) (Clarsen et al., 2014; Kibler et al., 2012; Kibler and McMullen, 2003; Struyf et al., 2011; Timmons et al., 2012). These abnormal movement patterns are often referred to as scapular dyskinesia (Kibler and Sciascia, 2010).

To prevent shoulder complaints in persons with SCI, early diagnosis and treatment of such movement disorders are required. However, in order to diagnose dyskinesia in persons with SCI, the normal movement pattern of the scapula and shoulder complex need to be well understood in this population.

During frontal-plane arm elevation, the movement pattern of the scapula is well described in an able-bodied population. With increasing TH elevation, the scapula tilts posteriorly and rotates laterally with respectively 0.1° (SD 0.03°) and 0.3° (SD 0.1°) per ° of elevation (Barnett et al., 1998; de Groot et al., 1999; Forte et al., 2009; Kijima et al., 2015; Lawrence et al., 2014; Lee et al., 2013; Ludewig et al., 1996; Matsuki et al., 2011; McClure et al., 2001; van den Noort et al., 2014, 2015).

During manual wheelchair propulsion, the kinematics of the GH joint have been described elaborately in both able-bodied subjects and persons with SCI (Acosta et al., 2001; Forte et al., 2009; Jahanian et al., 2016; Koontz et al., 2002; McClure et al., 2001; Rao et al., 1996). However the movement pattern of the scapula has not been described with sufficient consistency in these populations. To better understand these kinematics in actual wheelchair users and more closely designate the roles of either pathology or training in the development of shoulder problems, a description in able-bodied subjects is helpful and thus the primary aim of this study. In able-bodied subjects, no confounding alterations are expected as may be prevalent in SCI subjects due to muscle paralysis or postural changes. Hence the primary aim of the study is to describe the kinematics of the scapula during manual wheelchair propulsion in able-bodied persons.

The secondary aims are firstly to describe the kinematics of the total shoulder complex during a static position, arm elevation in the frontal plane and during low-intensity manual wheelchair propulsion and secondly to investigate the scapular movement pattern and the kinematics of the thorax, SC joint, AC joint and GH joint and arm segment lengths during the push phase of manual wheelchair propulsion.

2. Methods

2.1. Study participants

Sixteen able-bodied participants, novel to manual wheelchair propulsion, (10 males, 6 females) with a mean age of 25.4 years (SD 8.3), mean body mass of 71.1 kg (SD 13.8) and mean height of 1.79 m (SD 0.09), voluntarily participated in this study. Exclusion criteria were any prior experience with manual wheelchair propulsion, intensive regular upper-body exercise or medical contra-indications according to the 7-item Physical Activity Readiness Questionnaire (ACSM, 2009). All participants were informed about the nature of the study before giving written informed consent.

The local ethics committee of the Centre for Human Movement Sciences, University Medical Centre Groningen, University of Groningen, the Netherlands approved the study protocol.

2.2. Protocol

Prior to the experiment, the air-filled tires on both wheels of the experimental, handrim-propelled wheelchair (12 kg, 24-in. wheels,

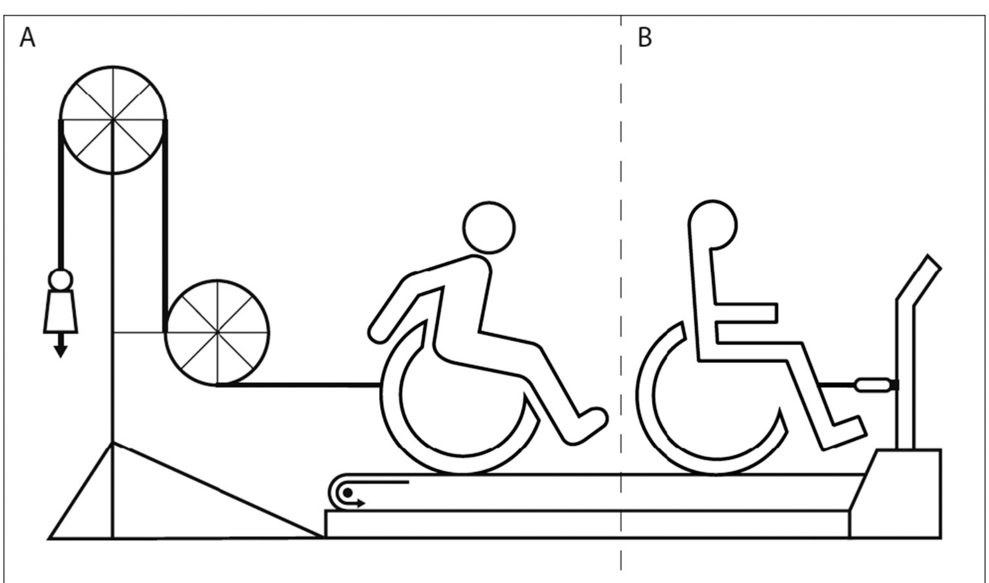

Fig. 1. A schematic overview of the experimental setup with the pulley system to reinforce the desired external power output (A) and the drag test, performed to determine the rolling resistance of the experimental wheelchair with the subject seated in it (B). Image adopted with permission from (Vegter et al., 2013).

Double Performance BV, Gouda, the Netherlands) were inflated to $6 \cdot 10^5$ Pa. with the participant seated in it. Active infrared cluster markers were attached to the upper body. The position of the upper-body in the anatomic posture was measured, while the participant was seated in a manual wheelchair. A drag test was performed to individually determine the rolling resistance (van der Woude et al., 1986) (Fig. 1B).

Subsequently, a standardized arm elevation movement in the frontal plane was performed at self-selected speed; seated in the wheelchair, the subjects were instructed to raise their arm from the hanging resting position until the arm was horizontal. After that, participants propelled their chair on a level motorized treadmill (Forcelink BV, Culemborg, the Netherlands) at 1.1 m/s. Each subject performed manual wheelchair propulsion during three steady-state 4-min trials, with 2-min rest intervals. The power-output was fixed at 0.20 W per kg body mass (the individuals calculated rolling resistance with the addition of a calculated mass using a pulley system (Veeger et al., 1989) (Fig. 1A)).

2.3. Instrumentation

2.3.1. Kinematic data collection

Three-dimensional positions of the trunk and the right arm were collected using an optoelectric camera system (Optotrak, Northern Digital, Waterloo, Canada) at 100 Hz. Technical cluster markers were attached to the right side of the participants' body on the back of the hand, dorsal wrist, distal humerus, sternum and on the wheelchair. A technical cluster marker placed on the acromion processus was used to track the motion of the scapula (van Andel et al., 2009) (Fig. 2).

Thirteen bony landmarks, with the addition of the second and fifth metacarpal joints and the ventral AC joint, were probed using a pointer during calibration measurements to define their position relative to their cluster markers (Wu et al., 2005).

2.3.2. Experimental wheelchair

The right rear wheel of the wheelchair was replaced with one of two instrumented wheels, either a Smartwheel (Three Rivers Holding LLC, Mesa, USA) or an Optipush (Max Mobility LCC, Antioch, USA), while the left rear wheel was replaced with a dummy wheel of similar weight, size and inertial characteristics. The start of the kinematic and kinetic data collection was electronically synchronised.

2.4. Data reduction and analysis

One representative arm elevation cycle, from the resting position to the maximum amplitude and back to the resting position, was selected per subject.

Four consecutive, representative propulsion cycles from the last minute of the third four-minute block were selected for each subject. A propulsion cycle was defined as a push phase, (the period of positive torque around the z-axis of the wheel > 1 Nm) and a recovery phase, (the period between the end of a push phase and the start of the consecutive push phase).

Motion data was converted to LCS of the thorax, scapula, humerus and forearm according to the ISB guidelines (Wu et al., 2005), with exception of a deviating LCS definition of the clavicle. This was done to account for axial rotation of the SC joint, under the assumption of minimal AC rotation (van der Helm and Pronk, 1995). The LCS of the clavicula was defined as: z-axis as vector from the SC joint to ACD; the y-axis as the vector perpendicular to the plane formed by ACD, ACV and SC, pointing cranially and the x-axis as the vector perpendicular to the y-axis and z-axis, pointing ventrally.

Using these calibrations, the three-dimensional coordinates of the bony landmarks were reconstructed during the experiment. Subsequently, a linear regression method was used to calculate the rotation centre of the glenohumeral joint (GH) (Meskers et al., 1998). Landmarks were low-pass filtered (zero-phase, 10 Hz, 2nd order Butterworth). Subsequently, Euler angles were calculated. For clarity, the thoracohumeral joint (TH) and GH elevation angles (negative according to ISB definition) are presented as positive values.

The segment length of the humerus was defined as distance between the midpoint of the medial and lateral humeral epicondyles of the humerus and the GH joint. The length of the ulna was defined as the distance between the medial humeral epicondyle and the ulnar styloid processes. Total arm length was the sum of the humeral and ulnar length. The distance between the spines of the seventh cervical vertebra and the eighth thoracic vertebra was taken as indicator of the length of the thorax.

Kinetic data were low-pass filtered (zero-phase, 10 Hz, 2nd order Butterworth) and re-sampled from 200 Hz to 100 Hz using a cubic spline.

2.5. Statistics

2.5.1. Descriptive statistics

Group means and standard deviations were calculated for the Euler angles of the upper body during the static pose in the anatomical posture, from 30° to 80° of arm elevation in 10° intervals (both ad- and abduction).

The mean angles and ranges were calculated for four consecutive push-phases, and subsequently the mean joint angles, mean ranges and coefficient of variation (CV) were calculated per-participant. A range of a push was defined as the absolute maximum value minus the absolute minimum value of a rotation.

2.5.2. Multilevel model definition

In order to perform an in-depth analysis of the relationship between the scapular motion pattern and the orientation of the thorax, humerus and clavicula during the push phase of manual wheelchair propulsion, multilevel regression analysis was performed to account for both inter- and intra-individual variances. Statistical analyses were performed, using the statistical programme “R” version 3.2.3 (R Core Team, 2013) and the packages “lme4” version 1.1–9 (Bates et al., 2015) and “irr” version 0.84 (Gamer et al., 2015).

Datasets of fourteen participants, containing four consecutive push-phases during the third four-minute block, were randomly selected out

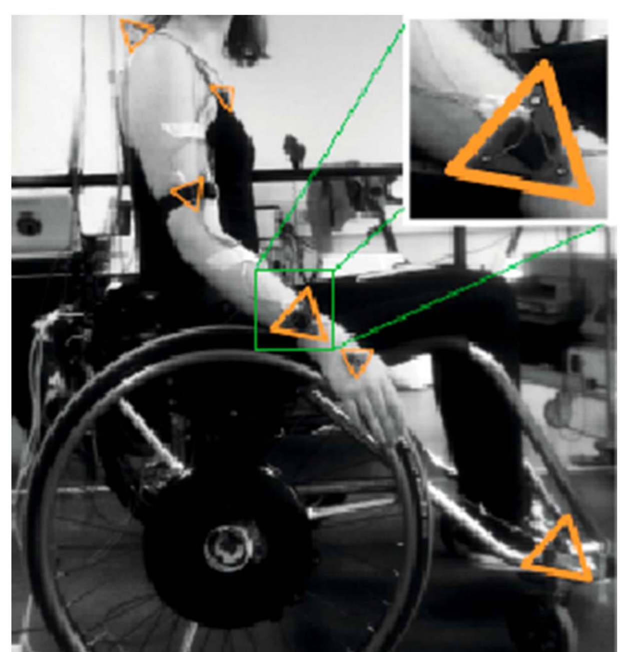

Fig. 2. Placement of the technical cluster markers (orange triangles) on the subjects' right acromion processus, caudal sternum, distal humerus, distal forearm, hand and experimental wheelchair. Image adopted with permission from (Vegter et al., 2015).

of the sixteen available datasets to define the multilevel models. The remaining two datasets were used for the validation of the multilevel models. In total, three models were defined for the three movements of the scapula relative to the thorax, respectively scapular protraction/retraction, lateral/medial rotation and anterior/posterior tilt. The orientations of the thorax, SC joint and TH joint, the lengths of the thorax and arm segments and the moments around the GH joint were first studied univariately in relation to the three scapular rotations. All variables that related significantly ($p < 0.05$) in the univariate analysis were used for the multivariate models. Using backward regression, one-by-one, non-significant terms were removed to reach the final models. The maximum likelihood estimation and coefficient of determination (r^2 value) were used to quantify the fit and the quality of the models respectively. The p-value of the maximum likelihood estimation was obtained using the chi-square distribution; r^2 was defined as: $r^2 = 1 -$ (residual variance)/(total model variance).

SC axial rotation was not included in the multilevel models, since the forward pointing axis of the clavicula is defined by the ventral and dorsal AC joints. These landmarks are defined in the cluster marker of the scapula. Therefore, by definition, a strong relation between SC axial rotation and scapular motion is expected.

2.5.3. Multilevel model validation

The two datasets, out of the sixteen available, that were not selected to define the models, were used to validate the multilevel models. The quality of the models was expressed by the ICC between measured and estimated data and the RMSE of the differences between the measured and estimated data for each of the remaining subsets.

3. Results

3.1. Scapular kinematics in a standardized static pose

In the anatomical posture, 34.7° (SD 5.3°) of protraction, 6.8° (SD 9.2°) of lateral rotation and 9.3° (SD 5.8°) of anterior tilt were observed at 18.7° (SD 10.0°) of TH elevation. See Table 2 for a full overview of the upper body kinematics in all tasks.

3.2. Scapular kinematics during arm elevation

At 80°of TH elevation in the frontal plane, scapular protraction and anterior tilt were respectively 33.4° (SD 8.0°) and 4.1° (SD 11.3°), lateral rotation increased to 23.9° (SD 5.3°). See Table 2 for a full overview of the upper body kinematics at 40° and 80° of TH elevation and Fig. 3 for a detailed overview of the ST kinematics during arm elevation.

On average, the scapular kinematics during arm elevation were in agreement with earlier bone pin studies, showing comparable values for the ST kinematics of around 35° of protraction and no effect of elevation angle (Lawrence et al., 2014; McClure et al., 2001) in able-bodied, healthy participants. The current study found 11.8° (SD 8.3°) of lateral rotation at 40°of TH elevation, increasing to 23.9° (SD 5.4°) at 80° of TH elevation. Scapular posterior tilt was found to be −7.3° (SD 6.3°) at 40° of TH elevation, and up to −4.1° (SD 11.3°) at 80° of TH elevation and slightly increasing with increasing TH elevation angle. Both the movement pattern and the values are comparable to the aforementioned studies.

3.3. Scapular kinematics during manual wheelchair propulsion

During the dynamic and relatively forceful push phase of manual wheelchair propulsion, the following one-push mean values of ST kinematics were found; 32.7° (SD 7.1°) for ST protraction, 7.1° (SD 9.2) for ST lateral rotation and 9.8° (SD 8.3°) for ST anterior tilt. Their respective ranges were of 15.6° (SD 5.2°), 8.8° (SD 7.5°) and 10.1° (SD 4.6°) (see Table 1). An overview of the ST kinematics during a mean, standardized propulsion cycle is shown in Fig. 4. On average, a push phase lasted for 38% of a full propulsion cycle at the belt speed of 1.11 m/s and 0.20 W/kg. The average power output was 16.4 W (SD 3.7 W). For the ST kinematics, coefficients of variations for inter-cycle variability for the absolute values were 0.02 for ST protraction, 0.24 for ST lateral rotation and 0.14 for ST anterior tilt, while the respective CV's for the push-ranges were 0.08, 0.14 and 0.08. All CV values can be found in Table 1.

3.3.1. Multilevel models

Multilevel models were defined based on fourteen out of sixteen randomly selected subsets describing submaximal, steady-state manual wheelchair propulsion. The univariate analysis showed that the axial rotation and lateral flexion of the thorax, the length of the thorax and external load around the GH joint did not contribute to the prediction of the scapular movement pattern, nor did the length of the individual arm segments (see Table 2).

Finding from the multivariate model for ST protraction indicate a strong negative association with forward flexion of the thorax and depression in the SC joint and a positive association with protraction of the SC joint and elevation of the TH joint. This model has an r^2 value of 0.67 and a RMSE of 2.42°.

The multivariate model for ST lateral flexion showed a strong positive relationship with forward flexion of the thorax and protraction and depression in the SC joint, but not with the elevation of the TH joint. The length of the arm does have a relationship with ST lateral rotation. The r^2 and RSME values were respectively 0.61 and 8.07°.

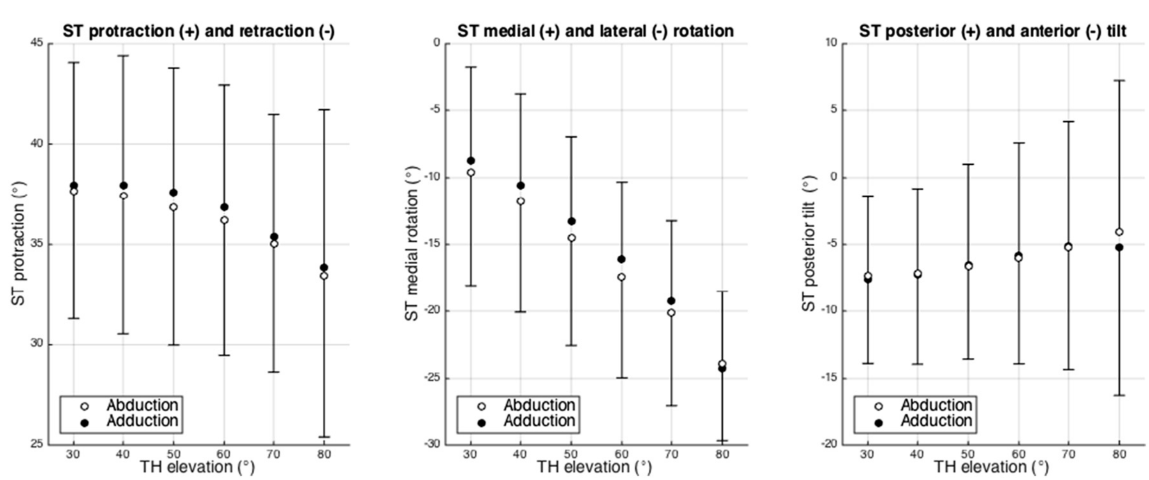

Fig. 3. Mean scapulothoracic joint (ST) kinematics during the ascending and descending phase of arm elevation (respectively abduction (∘) and adduction (•)) in the frontal plane, at 30° to 80° of thoracohumeral (TH) elevation ($N = 16$ except for 80° of TH elevation where $N = 14$). The vertical line indicates one standard deviation.

Table 1
Mean values and ranges of upper body kinematics during the static posture, arm elevation and manual wheelchair propulsion.

Joint		Static posture[1]		40° TH elevation				80° TH elevation				Manual wheelchair propulsion[2]					
				Abduction		Adduction		Abduction		Adduction		Means of 4 individual pushes			Ranges of 4 push phases		
		N = 16		N = 16		N = 16		N = 14[3]		N = 14[3]		*N* = 16			N = 16		
		Mean	(SD)	Mean	(SD)	Mean	(SD)	Mean	(SD)	Mean	(SD)	Mean	(SD)	CV	Mean	(SD)	CV
Thorax	Flexion	−8.5°	(6.2°)	−7.8°	(5.6°)	−8.1°	(6.2°)	−7.5°	(7.5°)	−7.8°	(7.9°)	−15.2°	(3.1°)	0.08	12.1	(4.8°)	0.07
	Lateral flexion	−1.1°	(1.9°)	−3.3°	(4.7°)	−2.6°	(4.8°)	−6.3°	(5.0°)	−5.7°	(5.0°)	−0.48°	(4.5°)	2.16	6.1°	(2.8°)	0.13
	Axial rotation	−3.7°	(4.8°)	−5.9°	(6.7°)	−5.9°	(6.4°)	−6.1°	(6.7°)	−5.9°	(7.0°)	−1.05°	(4.5°)	0.82	2.0°	(0.2°)	0.25
ST	Protraction	36.7°	(5.3°)	37.4°	(6.9°)	38.0°	(6.4°)	33.4 °	(8.0°)	33.8°	(7.9°)	32.7°	(7.1°)	0.02	15.6°	(5.2°)	0.08
	Lateral rotation	6.4°	(9.1°)	11.8°	(8.3°)	10.6°	(6.7°)	23.9°	(5.4°)	24.3°	(5.4°)	7.1°	(9.2°)	0.24	8.8°	(7.5°)	0.14
	Anterior tilt	−9.1°	(5.7°)	−7.3°	(6.3°)	−7.2°	(6.7°)	−4.1°	(11.3°)	−5.2°	(11.1°)	−9.8°	(8.3°)	0.14	10.1	(4.6°)	0.08
SC	Protraction	−18.1°	(9.7°)	−23.8°	(7.7°)	−24.2°	(7.4°)	−31.1°	(6.1°)	−31.5°	(6.4°)	−25.5°	(7.2°)	0.07	8.6°	(3.7°)	0.14
	Depression	−7.2°	(8.6°)	−9.9°	(6.5°)	−9.6°	(7.1°)	−16.2°	(5.3°)	−16.1°	(5.8°)	−9.4°	(7.1°)	0.08	4.6°	(3.4°)	0.18
	Backward rotation	−6.3°	(12.2°)	−2.1°	(12.2°)	−2.8°	(13.1°)	2.2°	(7.0°)	2.0°	(6.9°)	−9.6°	(4.1°)	0.14	18.4°	(1.2°)	0.02
AC	Protraction	42.5°	(3.2°)	43.0°	(3.6°)	43.4°	(3.4°)	44.4°	(2.4°)	44.2°	(2.5°)	42.8°	(4.1°)	0.02	2.1°	(2.5°)	0.31
	Medial rotation	−8.5°	(8.2°)	−2.3°	(5.2°)	−1.9°	(5.4°)	−3.6°	(2.4°)	−2.7°	(2.7°)	−4.2°	(8.4°)	0.31	4.1°	(3.8°)	0.21
	Posterior tilt	−0.6°	(6.1°)	−1.5°	(6.3°)	−1.2°	(6.2°)	5.1°	(6.2°)	3.8°	(5.3°)	4.5°	(6.4°)	0.13	3.1°	(5.1°)	0.28
GH	Plane of elevation	13.0°	(11.5°)	−9.54°	(16.4°)	−5.8°	(12.0°)	−26.1°	(12.8°)	−22.5°	(10.0°)	−11.2°	(24.2°)	0.12	80.4°	(15.3°)	0.01
	Elevation	−18.7°	(10.0°)	−27.9°	(7.5°)	−28.9°	(6.5°)	−56.7°	(6.7°)	−55.4°	(5.9°)	−38.4°	(9.1°)	0.44	14.3°	(3.2°)	0.06
	Internal rotation	−6.0°	(16.6°)	−12.4°	(8.3°)	−13.0°	(9.4°)	- 18.9°	(10.0°)	−19.1°	(8.7°)	21.4°	(21.4°)	0.14	22.8°	(13.1°)	0.01
TH	Plane of elevation	14.1°	(9.5°)	20.0°	(18.2°)	23.6°	(16.3°)	8.7°	(13.9°)	11.9°	(11.7°)	−16.1°	(28.1°)	0.07	79.1°	(16.2°)	0.01
	Elevation	−9.4°	(8.2°)	−40.0°	(0.1°)	−40.0°	(0.0°)	−80.0°	(0.0°)	−80.0°	(0.1°)	−41.2°	(10.7°)	0.05	12.9°	(3.8°)	0.06
	Internal rotation	−8.3°	(12.7°)	−14.8°	(8.0°)	−15.1°	(9.8°)	−21.9°	(7.9°)	−22.8°	(6.9°)	24.1°	(22.8°)	0.04	25.2°	(15.3°)	0.03

TH = thoracohumeral joint, CV = coefficient of variation, SD = standard deviation, ST = scapulothoracic joint, SC = sternoclavicular joint, AC = acromioclavicular joint, GH = glenohumeral joint.
[1] Static posture = sitting in a standardized posture in the experimental wheelchair, in the anatomical position.
[2] Manual wheelchair propulsion was performed at v = 1.11 m/s on a level treadmill at 16.3 W (SD 3.7 W).
[3] Two participants did not reach 80° of TH elevation.

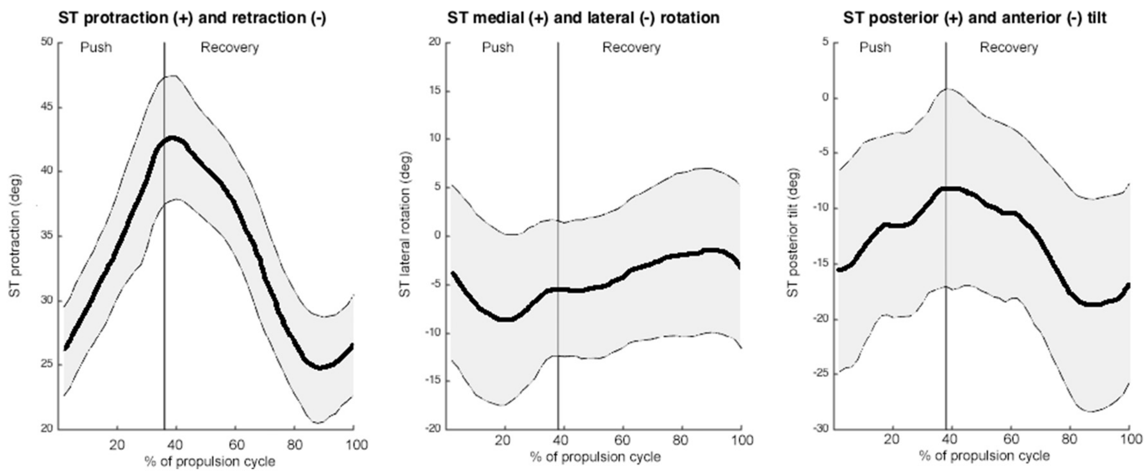

Fig. 4. Mean scapulothoracic joint (ST) kinematics during a standardized manual wheelchair propulsion cycle (time normalized) on a motor driven treadmill (v = 1.11 m/s, PO = 16.4 W (SD 3.7 W). The bold line indicates the mean of all per-participant means over 4 complete propulsion cycles. The grey area encloses one standard deviation from the mean. On average, a push-phase was 38% of the complete propulsion cycle.

The last multivariate model, for ST posterior tilt, showed positive relations with protraction in the SC joint and the plane of elevation of the TH joint.

For the model validation on two subsets, the ICC and RMSE values of the model-predicted data and measured data were calculated. The ICC and RMSE for ST protraction for the first and second dataset were respectively ICC = 0.82 ($p < 0.01$, RMSE 4.45°) and ICC = 0.76 ($p < 0.01$, RMSE 4.21°), for ST medial rotation ICC = 0.68 ($p < 0.01$, RMSE 6.59°) and ICC = 0.76 ($p < 0.01$, RMSE 5.18°) and for ST anterior tilt ICC = 0.63 ($p < 0.01$, RMSE 6.87°) and ICC = 0.69 ($p < 0.05$, RMSE 7.63°). The RMSE values are in the same order of magnitude as the RMSE of the multilevel models and the ICC values are acceptable, indicating an acceptable predictive value of the models.

4. Discussion

The current study provided a detailed description of the scapula's orientation in a static position and its movement pattern during frontal-plane arm elevation and manual wheelchair propulsion in a group of novices. This description will further aid in the understanding and interpretation of the scapular behaviour in wheelchair users, e.g. persons with an SCI, and in the context of the development of shoulder problems in this population.

4.1. Static pose in anatomical position

To put the current study into context, the study of Ludewig and colleagues described the resting position of the scapula in able-bodied participants, measured with bone-fixed sensors, in a standardized position with the arm along the participant's side (Ludewig et al., 2009). Transformed into Euler angles in the ISB proposed format, their findings were 41.1° (SD 2°) of protraction, 5.4° (SD 1°) of lateral rotation and 13.5° (SD 2°) of anterior tilt. The difference with the current study could be due to the differences in instrumentation used; in the current study, skin mounted cluster markers were used to measure the position of the scapula and thorax in contrast to bone-fixed sensors in the study of Ludewig and colleagues. The observed differences are within the RMSE values found in a validation study between the ACM and bone-fixed sensors (Karduna et al., 2001).

Even though the ACM can be inaccurate due to soft-tissue artefacts, errors in positioning and a varying centre of rotation of the scapula (Ludewig et al., 1996), the ACM has been shown to be both reliable (Haik et al., 2014; Warner et al., 2015) and valid in healthy, able-bodied participants in comparison to bone-fixed sensors and radiological measures (Lempereur et al., 2014). Since the use of the non-invasive ACM does allow for unrestrained movement and is a reliable and valid instrument, it has been used in the current study. To minimize systematic error, one researcher performed all palpations.

4.2. Scapular kinematics during arm elevation

On average, the scapular kinematics during arm elevation were in agreement with earlier bone pin studies, showing comparable values for the ST kinematics of around 35° of protraction and no effect of elevation angle (Lawrence et al., 2014; McClure et al., 2001) in able-bodied, healthy participants. The current study found 11.8° (SD 8.3°) of lateral rotation at 40°of TH elevation, increasing to 23.9° (SD 5.4°) at 80° of TH elevation. Scapular posterior tilt was found to be −7.3° (SD 6.3°) at 40° of TH elevation, and up to −4.1° (SD 11.3°) at 80° of TH elevation and slightly increasing with increasing TH elevation angle. Both the movement pattern and the values are comparable to the aforementioned studies.

Table 2
Multilevel models for the prediction of the 3D scapular motion pattern from the position of the thorax and arm ($N = 14$). Shown are the coefficients of the final models with their respective r^2, p-values and RMSE. Data from 14 randomly selected subsets, containing 4 consecutive push-phases of manual wheelchair propulsion, were used to define the models.

ST joint	Intercept	Thorax			SC joint		TH joint			Segment lengths				P [a]	r^2 [b]	RMSE
		Flexion	Lat rot	Ax rot	Protr	Depr	Elev	Pl. elev	Int rot	Thorax	Hum	Ulna	Arm			
Protraction	40.02	−0.12	/	/	0.51	−0.39	0.07	/	/	/	/	/	/	< 0.001	0.67	2.42°
Lateral rotation	−12.1	0.58	/	/	0.81	0.94	/	–	–	/	/	/	0.00012	< 0.001	0.61	8.07°
Posterior tilt	2.98	/	/	/	0.33	/	/	0.05	/	/	/	/	/	< 0.01	0.52	7.44°

/ = term was eliminated in the univariate analysis; − = term was eliminated in the backwards regression; [a] = p-value was calculated according the chi-square distribution, comparing the maximum-likelihood statistic of the final model to the initial model; [b] = r^2 was defined as: 1 - r^2 = (residual variance)/(total model variance).
RMSE = root mean square error; SC = sternoclavicular; TH = thoracohumeral; ST = scapulothoracic.

4.3. Scapular kinematics during manual wheelchair propulsion

During wheelchair propulsion at 1.1 m/s, the ST and GH kinematics, both the movement patterns and ranges showed similarities to the study of Zhao and colleagues (Zhao et al., 2015). In that study, the ST and GH movement pattern is described in persons with SCI (both tetraplegia and paraplegia, 13 M 2F, 39 years of age (SD 12 years), 14 years of wheelchair use (SD 9 years)) with mild to moderate shoulder pain during wheelchair propulsion. However, the velocity of wheelchair propulsion and exact mean rotation values and their ranges were not specified in their study. Even though no exact values are given in the study of Zhao and colleagues, the values for ST protraction and ST medial rotation in the current study appear to be systematically higher over a propulsion cycle and ST posterior tilt appears to be lower.

The study of Roux and colleagues (Roux et al., 2006) described manual wheelchair propulsion in novice, able-bodied participants at 1.1 m/s and found a mean range of 31.3° (SE 3.3°) of ST protraction, 8.7° (SE 1.5°) of lateral rotation and 13.7° (SE 1.4°) of posterior tilt. However, these values are calculated using the YZ′X″ decomposition order. Expressed in the ISB recommended YX′Z″ decomposition format, these values are respectively 33.3° of protraction, 13.5° of lateral rotation and 9.0° of posterior tilt.

The study of Koontz and colleagues (Koontz et al., 2002) described GH kinematics during manual wheelchair propulsion in persons with paraplegia (17 M 10F, 36 years of age (SD 10 years), 11 years of wheelchair use (SD 5 years)) at 0.9 m/s and 1.8 m/s on a dynamometer. However, comparison is difficult due to a different definition of the TH orientations and matrix decomposition order, however a mean TH elevation angle of 42° and a range of around 16° of humeral elevation as well a range of 28° humeral internal rotation are in agreement with the current study.

Even though the study of Rao and colleagues did not describe the ST joint kinematics, it does allow for comparison of CV values, GH kinematics and forward flexion of the thorax (Rao et al., 1996). The persons with low-level paraplegia in this study seemed to use the same motion ranges of GH elevation plane and elevation, but more humeral internal rotation, possibly due to different propulsion techniques, as a result of training and skill.

4.3.1. Multilevel models

In general, the current multilevel models show similar r^2 and RMSE values as prior studies (de Groot and Brand, 2001; Grewal and Dickerson, 2013; Veeger et al., 1993). In their study, de Groot and Brand developed a model based on various static orientations, both with and without external loading while the study of Grewal and Dickerson developed a model based on arm elevation in different planes. This could limit the applicability and therefore comparability to manual wheelchair propulsion. The model of Veeger and colleagues on the other hand was based on a simulated wheelchair push under static conditions.

In contrast to earlier research (de Groot and Brand, 2001; Grewal and Dickerson, 2013) no relations were found in the final models between the humeral elevation angle and the motion of the scapula during arm elevation. This could be due to the different nature of the wheelchair push where the humeral elevation is typically low and with a limited range, between 30° and 60° (Feng et al., 2010; Rao et al., 1996). The models as defined by de Groot and Brand as well as by Grewal and Dickerson involved TH elevation angles up to 180°. Therefore, the multilevel models as defined in this study should be used with caution, when applied to motions with higher expected elevation ranges.

4.4. Implications

Further research on scapular kinematics and its relation to shoulder pathology in manual wheelchair dependent populations can profit of these findings as reference values. It will allow a detailed comparison of scapular kinematics in a wheelchair dependent population to the able-bodied population.

5. Conclusion

The normal movement pattern of the scapula has been described in a static pose and during arm elevation and manual wheelchair propulsion in able-bodied persons. The movement pattern shows good comparability to earlier studies in able-bodied and persons with SCI, but absolute values differ for ST protraction and ST anterior tilt.

These findings can provide further support in the understanding of normal and altered upper body kinematics in persons with limited upper-body function, for example persons with a spinal cord injury.

Conflict of interest

All authors declare no conflict of interest.

Acknowledgements

We like to thank all the participants for their cooperation in the study. We thank all the bachelor students of the Center for Human Movement Sciences involved in the data collection. Furthermore, we like to thank the technical support department of the Center for Human Movement Sciences for their assistance and expertise during the preparation and execution of the experiment. Finally we thank Anne Buzzell from the Swiss Paraplegic Research for proof reading the manuscript.

Contributions

MB contributed to participant recruitment, data collection, data analysis, interpretation of the results and writing the manuscript.

RJKV contributed to the design and set-up of the study and the data collection.

JWvdS contributed to the design and set-up of the study and the data collection.

JH contributed to the design and set-up of the study, participant recruitment and the data collection.

SdG contributed to the design and set-up of the study.

WdV contributed to writing the manuscript.

UA contributed to the analysis and interpretation of the results and writing the manuscript.

LHVvdW contributed to the design and set-up of the study and to the interpretation of the results and writing the manuscript.

HEJV contributed to the analysis and interpretation of the results and writing the manuscript.

References

Acosta, A.M., Kirsch, R.F., van der Helm, F.C.T., 2001. Three-dimensional shoulder kinematics in individuals with C5-C6 spinal cord injury. Proc. Inst. Mech. Eng. H J. Eng. Med. 215, 299–307.

ACSM, 2009. ACSM's Guidelines for Exercise Testing and Prescription, eighth edition.

Ballinger, D.A., Rintala, D.H., Hart, K.A., 2000. The relation of shoulder pain and range-of-motion problems to functional limitations, disability, and perceived health of men with spinal cord injury: a multifaceted longitudinal study. Arch. Phys. Med. Rehabil. 81, 1575–1581.

Barnett, N.D., Duncan, P., Johnson, G.R., 1998. The measurement of three dimensional scapulohumeral kinematics - a study of reliability. Clin. Biomech. 14.

Bates, D., Maecher, M., Bolker, B., Walker, S., Christensen, R.H.B., Singmann, H., Dai, B., Grothendieck, G., 2015. Linear Mixed-effects Models Using 'Eigen' and S4 (R Pacakge 'lme4).

Clarsen, B., Bahr, R., Andersson, S.H., Munk, R., Myklebust, G., 2014. Reduced glenohumeral rotation, external rotation weakness and scapular dyskinesis are risk factors for shoulder injuries among elite male handball players: a prospective cohort study. Br. J. Sports Med. 48, 1327–1333.

Curtis, K.A., Roach, K.E., Applegate, E.B., Amar, T., Benbow, C.S., Genecco, T.D., Gualano, J., 1995. Development of the wheelchair User's shoulder pain index (WUSPI). Paraplegia 33, 290–293.

de Groot, J.H., Brand, R.A., 2001. A three-dimensional regression model of the shoulder rhythm. Clin. Biomech. 16, 735–743.
de Groot, J.H., van Woensel, W., van der Helm, F.C., 1999. Effect of different arm loads on the position of the scapula in abduction postures. Clin. Biomech. 14, 309–314.
Eriks-Hoogland, I.E., de Groot, S., Post, M.W., van der Woude, L.H., 2011. Correlation of shoulder range of motion limitations at discharge with limitations in activities and participation one year later in persons with spinal cord injury. J. Rehabil. Med. 43, 210–215.
Feng, C.K., Wei, S.H., Chen, W.Y., Lee, H.C., Yu, C.H., 2010. Comparing the shoulder impingement kinematics between circular and pumping strokes in manual wheelchair propulsion. Disabil. Rehabil. Assist. Technol. 5, 448–455.
Finley, M.A., McQuade, K.J., Rodgers, M.M., 2005. Scapular kinematics during transfers in manual wheelchair users with and without shoulder impingement. Clin. Biomech. 20, 32–40.
Forte, F.C., de Castro, M.P., de Toledo, J.M., Ribeiro, D.C., Loss, J.F., 2009. Scapular kinematics and scapulohumeral rhythm during resisted shoulder abduction–implications for clinical practice. Phys. Ther. Sport 10, 105–111.
Gamer, M., Lemon, J., Fellows, I., Singh, P., 2015. Various Coefficients of Interrater Reliability and Agreement (R Package 'irr').
Gironda, R.J., Clark, M.E., Neugaard, B., Nelson, A.L., 2004. Upper limb pain in a national sample of veterans with paraplegia. J. Spinal Cord Med. 27, 120–127.
Grewal, T.J., Dickerson, C.R., 2013. A novel three-dimensional shoulder rhythm definition that includes overhead and axially rotated humeral postures. J. Biomech. 46, 608–611.
Haik, M.N., Alburquerque-Sendin, F., Camargo, P.R., 2014. Reliability and minimal detectable change of 3-dimensional scapular orientation in individuals with and without shoulder impingement. J. Orthop. Sports Phys. Ther. 44, 341–349.
Jahanian, O., Schnorenberg, A.J., Brooke, A.S., 2016. Evaluation of shoulder joint kinematics and muscle activity during geard and standard manual wheelchair mobility. Conf. Proc. IEEE Eng. Med. Biol. Soc. 6162–6165.
Karduna, A.R., McClure, P.W., Michener, L.A., Sennett, B., 2001. Dynamic measurements of three-dimensional scapular kinematics: a validation study. J. Biomech. Eng. 123, 184.
Kibler, W.B., McMullen, J., 2003. Scapular kinematics and its relation to shoulder pain. J. Am. Acad. Orthop. Surg. 11, 142–151.
Kibler, W.B., Sciascia, A., 2010. Current concepts: scapular dyskinesis. Br. J. Sports Med. 44, 300–305.
Kibler, W.B., Sciasia, A., Wilkes, T., 2012. Scapular Dyskinesis and its relation to shoulder injury. J. Am. Acad. Orthop. Surg. 20, 364–372.
Kijima, T., Matsuki, K., Ochiai, N., Yamaguchi, T., Sasaki, Y., Hashimoto, E., Sasaki, Y., Yamazaki, H., Kenmoku, T., Yamaguchi, S., Masuda, Y., Umekita, H., Banks, S.A., Takahashi, K., 2015. In vivo 3-dimensional analysis of scapular and glenohumeral kinematics: comparison of symptomatic or asymptomatic shoulders with rotator cuff tears and healthy shoulders. J. Shoulder Elb. Surg. 24, 1817–1826.
Koontz, A.M., Cooper, R.A., Boninger, M.L., Souza, A.L., Fay, B.T., 2002. Shoulder kinematics and kinetics during two speeds of wheelchair propulsion. J. Rehabil. Res. Dev. 36, 635–650.
Lawrence, R.L., Braman, J.P., Laprade, R.F., Ludewig, P.M., 2014. Comparison of 3-dimensional shoulder complex kinematics in individuals with and without shoulder pain, part 1: sternoclavicular, acromioclavicular, and scapulothoracic joints. J. Orthop. Sports Phys. Ther. 44 (636–645), a631–638.
Lee, S.K., Yang, D.S., Kim, H.Y., Choy, W.S., 2013. A comparison of 3D scapular kinematics between dominant and nondominant shoulders during multiplanar arm motion. Indian J. Orthop. 47, 135–142.
Lempereur, M., Brochard, S., Leboeuf, F., Remy-Neris, O., 2014. Validity and reliability of 3D marker based scapular motion analysis: a systematic review. J. Biomech. 47, 2219–2230.
Ludewig, P.M., Cook, T.M., Nawoczenski, D.A., 1996. Three-dimensional scapular orientation and muscle activity at selected positions of humeral elevation. J. Orthop. Sports Phys. Ther. 25, 57–65.
Ludewig, P.M., Phadke, V., Braman, J.P., Hassett, D.R., Cieminski, C.J., LaPrade, R.F., 2009. Motion of the shoulder complex during multiplanar humeral elevation. J. Bone Joint Surg. Am. 91, 378–389.
Luime, J.J., Koes, B.W., Hendriksen, I.J.M., Burdorf, A., Verhagen, A.P., Miedema, H.S., Verhaar, J.A.N., 2004. Prevalence and incidence of shoulder pain in the general population; a systematic review. Scand. J. Rheumatol. 33, 73–81.
Matsuki, K., Matsuki, K.O., Mu, S., Yamaguchi, S., Ochiai, N., Sasho, T., Sugaya, H., Toyone, T., Wada, Y., Takahashi, K., Banks, S.A., 2011. In vivo 3-dimensional analysis of scapular kinematics: comparison of dominant and nondominant shoulders. J. Shoulder Elb. Surg. 20, 659–665.
McClure, P.W., Michener, L.A., Sennett, B.J., Karduna, A.R., 2001. Direct 3-dimensional measurement of scapular kinematics during dynamic movements in vivo. J. Shoulder Elb. Surg. 10, 269–277.
Meskers, C.G.M., van der Helm, F.C.T., Rozendaal, L.A., Rozing, P.M., 1998. In vivo estimation of the glenohumeral joint rotation center from scapular bony landmarks by linear regression. J. Biomech. 31, 93–96.
R Core Team, 2013. R: a Language and Environment for Statistical Computing. R Foundation for Statistical Computing, Vienna, Austria.
Rao, S.S., Bontrager, E.L., Gronley, J.K., Newsam, C.J., Perry, J., 1996. Three-dimensional kinematics of wheelchair propulsion. IEEE Trans. Rehabil. Eng. 4, 152–160.
Roux, L., Hanneton, S., Roby-Brami, A., 2006. Shoulder movements during the initial phase of learning manual wheelchair propulsion in able-bodied subjects. Clin. Biomech. 21, S45–S51.
Salisbury, S.K., Choy, N.L., Nitz, J., 2003. Shoulder pain, range of motion, and functional motor skills after acute tetraplegia. Arch. Phys. Med. Rehabil. 84, 1480–1485.
Samuelsson, K.A., Tropp, H., Gerdle, B., 2004. Shoulder pain and its consequences in paraplegic spinal cord-injured, wheelchair users. Spinal Cord 42, 41–46.
Struyf, F., Nijs, J., Baeyens, J.P., Mottram, S., Meeusen, R., 2011. Scapular positioning and movement in unimpaired shoulders, shoulder impingement syndrome, and glenohumeral instability. Scand. J. Med. Sci. Sports 21, 352–358.
Timmons, M.K., Thigpen, C.A., Seitz, A.L., Karduna, A.R., Arnold, B.L., Michener, L.A., 2012. Scapular kinematics and Subacromial-impingement syndrome: a meta-analysis. J. Sport Rehabil. 21, 354–370.
Turner, J.A., Cardenas, D.D., Warms, C.A., McClellan, C.B., 2001. Chronic pain associated with spinal cord injuries: a community survey. Arch. Phys. Med. Rehabil. 82, 501–509.
van Andel, C., van Hutten, K., Eversdijk, M., Veeger, H.E.J., Harlaar, J., 2009. Recording scapular motion using an acromion marker cluster. Gait Posture 29, 123–128.
van den Noort, J.C., Wiertsema, S.H., Hekman, K.M., Schonhuth, C.P., Dekker, J., Harlaar, J., 2014. Reliability and precision of 3D wireless measurement of scapular kinematics. Med. Biol. Eng. Comput. 52, 921–931.
van den Noort, J.C., Wiertsema, S.H., Hekman, K.M., Schonhuth, C.P., Dekker, J., Harlaar, J., 2015. Measurement of scapular dyskinesis using wireless inertial and magnetic sensors: importance of scapula calibration. J. Biomech. 48, 3460–3468.
van der Helm, F.C.T., Pronk, G.M., 1995. Three dimensional recording and description of motions of the shoulder mechanism. J. Biomed. Eng. 177, 27–40.
van der Woude, L.H.V., de Groot, G., Hollander, A.P., van Ingen Schenau, G.J., Rozendaal, R.H., 1986. Wheelchair ergonomics and physiological testing of prototypes. Ergon. Des. 29, 1561–1573.
van Drongelen, S., de Groot, S., Veeger, H.E., Angenot, E.L., Dallmeijer, A.J., Post, M.W., van der Woude, L.H., 2006. Upper extremity musculoskeletal pain during and after rehabilitation in wheelchair-using persons with a spinal cord injury. Spinal Cord 44, 152–159.
Veeger, H.E.J., van der Woude, L.H.V., Rozendal, R.H., 1989. The effect of rear wheel camber in manual wheelchair propulsion. J. Rehabil. Res. Dev. 26, 37–46.
Veeger, H.E.J., van der Helm, F.C.T., Rozendal, R.H., 1993. Orientation of the scapula in a simulated wheelchair push. Clin. Biomech. 8, 81–90.
Vegter, R.J.K., Lamoth, C.J., de Groot, S., Veeger, H.E.J., van der Woude, L.H.V., 2013. Variability in bimanual wheelchair propulsion: consistency of two instrumented wheels during handrim wheelchair propulsion on a motor driven treadmill. J. Neuroeng. Rehabil. 10.
Vegter, R.J.K., de Groot, S., Lamoth, C.J., Hartog, J., Bekker, J.M., van der Scheer, J.W., van der Woude, L.H.V., Veeger, H.E.J., 2015. Early motor learning changes in upper-limb dynamics and shoulder complex loading during handrim wheelchair propulsion. J. Neuroeng. Rehabil. 10, 12–26.
Warner, M.B., Chappell, P.H., Stokes, M.J., 2015. Measurement of dynamic scapular kinematics using an acromion marker cluster to minimize skin movement artifact. J. Vis. Exp. e51717.
Wu, G., van der Helm, F.C.T., Veeger, H.E.J., Makhsous, M., van Roy, P., Anglin, C., Nagels, J., Karduna, A.R., McQuade, K., Wang, X., Werner, F.W., Buchholz, B., 2005. ISB recommendation on definitions of joint coordinate systems of various joints for the reporting of human joint motion—part II: shoulder, elbow, wrist and hand. J. Biomech. 38, 981–992.
Zhao, K.D., Van Straaten, M.G., Cloud, B.A., Morrow, M.M., An, K.N., Ludewig, P.M., 2015. Scapulothoracic and glenohumeral kinematics during daily tasks in users of manual wheelchairs. Front. Bioeng. Biotechnol. 3, 183.